Research Article

Immune Reaction Induced with Hapten Enhanced Intratumoral Chemotherapy during Esophagectomy: Explore Possible Immunosurgery

Baofa, Yu[1,2,3,4,5*], Jian Zhang[2], Hongzhu Gao[6], Han Yan[2], Feng Gao[1], Peng Jing[1], Peicheng Zhang[1], Guoqin Zheng[1], Xiaomin Zhang[1]

Abstract

Background: Surgery is one of the main treatments for esophageal cancer, which can rapidly reduce tumor burden. If the surgery can induce immune response and wake up immune cells, it may be possible to translate surgery into immunesurgery. It will be significantly improved by combining with immune therapy by hapten enhanced intratumoral chemotherapy (HEIC) during esophagectomy.

Methods: scRNA-seq was used to analyze and define the molecular and cellular identities in tumors before and followed hapten enhanced intratumor chemotherapy.

Results: Following hapten enhanced intratumoral chemotherapy (HEIC), 8 different cell types were identified in the tumor tissues: B cells, basophils, Ecs, epithelial cells, fibroblasts, MPs, neutrophils and TandNK, while 7 different cell types were found in the blood samples while in tumor immunity, $\gamma\delta T$ cells can migrate to the local tumor environment by recognizing NK cell surface receptors and directly kill tumors by releasing cytotoxic substances such asIFN-γ, TNF-α.

Conclusion: Immune surgery can be possible performed by intratumoral injection of hapten plus cytotoxic drugs during esophagectomy, indues the immune response for awake immune cells in the preparation of immunotherapy and prevention of tumor metastasis with or without PD1 or PD-l1.

Highlights: Single-cell RNA sequencing (scRNA-seq) is used to profile the immune reaction induced by hapten enhanced local chemotherapy. Important changes of the immune response followed by hapten-enhanced intratumoral chemotherapy (HEIC) are identified at both the cellular and molecular levels in the esophageal cancer tissue as well as in the patient's blood samples in short time of esophagectomy.

Keywords: Intratumoral injection; Cancer immunotherapy; Drug delivery; Intracellular drug delivery for surgery; Immune surgery.

Introduction

Surgery has been playing an important role in cancer treatment for more than 100 years ever since the beginning of cancer treatment [1]. Historically, the surgeon's spells has been that more and more aggressive surgery would improve the cure rate. Despite the past 50 years we have witnessed new technologies flourishing; surgery is the textbook treatment for cancer and remains to be the dominant method in oncology with no sign of change [1].

Affiliation:

[1]TaiMeiBaofa Cancer hospital, Dongping, Shandong Province, China, 271500

[2]Jinan Baofa Cancer hospital, Jinan, Shandong Province, China, 250000

[3]Beijing Baofa Cancer Hospital, Beijing, China, 100010

[4]Immune Oncology Systems, Inc, San Diego, CA, USA, 92102

[5]South China Hospital of Shenzhen University, Shenzhen, 518116, P. R. China,

[6]Jinan Huaiyin People Hospital

*Corresponding author:
Baofa Yu, TaiMeiBaofa Cancer hospital, Dongping, Shandong Province, China, 271500.

Chemotherapy and radiotherapy combined with surgery represents a significant breakthrough in treating tumors. Adjuvant chemotherapy and radiation therapy has been used to shrink tumors before surgery [2]. Intraoperative radiotherapy (IORT) also used for surgery. Although IORT did not prolong overall survival in patients with gastric and esophageal cancer, the method showed good local-regional control in patients with specific stages without increasing the risk of complications [3-5]. However, metastasis or residual tumor cells due to compression of tumor residuals during surgery remains a problem. As a result, in many cases, successful surgery doesn't always ensure successful treatment and prolong patient's life. In order to improve the long-term success rate of surgical treatment and prevent metastasis caused by local tumor residual and crush residual, it is expected to rapidly reduce tumor burden during esophagectomy and enhance immunosuppressive potential tumor metastasis by stimulating the body's specific immunity to residual cancer cells, which is closely followed by PD1 immunotherapy [6]. Hapten-enhanced intratumoral chemotherapy (HEIC) can kill tumors and induce an immune response, which can promote neoantigen presentation by stimulating the release of hapten-modified tumor-associated antigens [7-18]. HEIC can also enhance the function of CD4, CD8, DC and B cells [11-14, 17, 18]. The fusion of this method in surgery will play a role in awakening immune cells, help immunotherapy to recognize and kill tumors and PD1 immunotherapy, and realize the transformation of immunosurgery. HEIC has been applied in many cancer patients that are not suitable for surgical treatment and it has achieved good clinical effects and extended the survival time of patients [17, 19]. Although hapten immunotherapy has been studied as a potential cancer treatment, its effectiveness and safety are still the subject of debate and ongoing research. For example, some studies suggest that haptens can stimulate an immune response against cancer cells, while others suggest that the immune response may actually be directed against healthy tissue. Here, we discuss the application of HEIC in the treatment of esophageal cancer (EC). EC is one of the deadliest malignancies worldwide, with developing countries accounting for more than 80% of total cases and deaths [20]. With a dramatic increase in incidence in the Western world over the past few decades [19, 21], EC has become the eighth most common cancer and the sixth most common cause of death [22]. The prognosis of esophageal cancer is poor, and the detection, prediction and treatment methods of esophageal cancer need to be significantly improved [23]. In the current study, HEIC was fused into the surgical procedure to induce an acute immune response and prevent tumor metastasis and recurrence. Small piece of esophageal carcinoma tissues were surgically removed directly from the tumor at opening chest of surgery as control and another small piece esophageal carcinoma tissues at 1 hour later after HEIC injected into tumor of esophageal carcinoma. Blood samples were also taken from the patient before and after surgery. We then used single-cell RNA sequencing (scRNA-Seq) to obtain transcriptome profiles of 32918 cells. Through comparative analysis of control and treated samples of tumor and blood samples before and after surgery, we comprehensively described the expression characteristics of malignant epithelial cells and immune cells, including bone marrow cells, stromal cells, T cells, plasma cells, B cells, platelets, epithelial cells, as well as the dynamic changes in cell percentage and cell subtype heterogeneity. Our results have provided evidence for acute immune response in esophageal cancer tissues induced by intratumoral co-administration of hapten with chemotherapy drugs, supporting the clinical utility of HEIC as a potential cancer treatment.

Materials and Methods

Ethical Statement

All procedures and protocols in the study has been reviewed and approved by the Ethical Committee of the Beijing Baofa Cancer Hospital (TMBF 0010, 2015). All informed consent forms form patients have been signed prior to the start of the study.

Clinical Specimens

The patient had a pathological diagnosis and was determined to have a clinical stage of IIa (T1-2N0Mo) tumor (5cm x 3.5cm x1.5cm) at middle section of esophagus [24]. The patient did not have any other therapy before this study. Before receiving this treatment at Beijing Baofa Cancer Hospital, the patient's physical condition was evaluated and determined to be consistent with surgical correction and met the indications for HEIC. This experimental treatment was approved by the hospital ethics committee (TMBF 0010, 2015) in accordance with relevant guidelines and regulations.

After the patient has been prepared for operation, the skin was sterilized again under general anesthesia and a disinfecting towel is laid. When the tumor tissue was open to be seen by surgeon, a small piece of tumor tissue (2mm×2mm×3mm) was taken as an untreated sample for scRNA-Seq analysis; This was followed by intratumoral injection of a total of 5 ml that contained 1.00 mg/ml Adriamycin (Adr), 0.80 mg/ml of cytarabine (Ara-C), 20.0 mg/ml of H_2O_2 and 144 mg/ml of penicillin as the hapten. 1.5 hours post injection, surgeon prepared the blunt separation of tissue and esophageal tumor was totally removed, a small piece (2mm×2mm×3mm) of tumor tissue was taken again as the treated samples for scRNA-Seq analysis. There were several lymph nodes with metastasis. A total of eight blood samples from the patient was taken as well at before and 24 hours after injection, one and two weeks after treatment. The blood samples were also to be analyzed by scRNA-Seq.

Citation: Baofa, Yu, Jian Zhang, Hongzhu, Gao, Han Yan, Feng Gao, Peng Jing, Peicheng Zhang, Guoqin Zheng, Xiaomin Zhang. Immune Reaction Induced with Hapten Enhanced Intratumoral Chemotherapy during Esophagectomy:Explore Possible Immunosurgery. Journal of Cancer Science and Clinical Therapeutics. 8 (2024): 10-21.

Tissue Disassociation and Cells Collection

After surgically extracted (Figure 1c, d), the fresh tissue samples were immediately stored in the sCelLiVE® Tissue Preservation Solution (Singleron) on ice. The tissues were cut into small tissue pieces and were transferred to a 15-ml centrifuge tube, followed by digestion using sCelLiVE® Tissue Dissociation Solution (Singleron) at 37°C for 15 min with shaking. The samples were then filtered with 40 µm sterile strainers, and centrifuged at 1,000 rpm at 4°C for 5 min. Next, 2 ml GEXSCOPE® red blood cell lysis buffer (RCLB, Singleron) was added to lyse the red blood cells for 10 min. Finally, the single cell suspension was collected after re-suspension with PBS, and trypan blue (Sigma) staining was used to calculate cell activity and cell count under a microscope.

Single-Cell RNA Sequencing

Single-cell suspensions (1~3×105 cells/mL) in PBS (HyClone) were loaded onto microwell chip using the Singleron Matrix® Single Cell Processing System. Briefly, the scRNA-seq library was constructed using the GEXSCOPE® Single Cell RNA Library Kits (Singleron). The library was lastly sequenced with 150 bp was diluted to 4nM and paired-end reads on the IlluminaHiSeq X platform following an established protocol [25]. Sequencing data processing and quality control was performed as described in previous publications [24, 26].

Data Processing and analysis

To identify differentially expressed genes (DEGs), genes expressed in more than 10% of the cells were selected in both of the compared groups of cells and with an average log (fold changes) value greater than 1 as DEGs. The cell type identity of each cluster was determined with the expression of canonical markers found in the DEGs using SynEcoSys database (Singleron Biotechnologies). The InferCNV package was used to detect the CNAs in malignant cells. Non-malignant cells (T and NK cells) were used as control references to estimate the CNVs of malignant cells. Genes expressed in more than 20 cells were sorted based on their loci on each chromosome. The relative expression values were centered to 1, using 1.5 standard deviation from the residual-normalized expression values as the ceiling.

To investigate the potential functions of DEGs between clusters, the Gene Ontology (GO) and Kyoto Encyclopedia of Genes and Genomes (KEGG) analysis were used with the "clusterProfiler" R package 3.16.1 [27]. Monocle 2 algorithm was used for pseudo-time trajectory analysis, and the dimensionality reduction method used was DDRTree [28]. Intra-tumoral heterogeneity (ITH) score calculation: The ITH score was defined as the average Euclidean distance between the individual cells and all other cells, in terms of the first 20 principal components derived from the normalized expression levels of highly variable genes. Cell-cell interaction (CCI) between B cells, Epithelial cells, Fibroblasts, Mononuclear phagocytes, Mast cells, Neutrophils, T and NK cells were predicted based on known ligand–receptor pairs by Cellphone DB v2.1.0 [29, 30].

Results

Clinical Benefit Characteristics

After surgery, pathology showed squamous cell carcinoma same as diagnosis earlier and no metastasis was found in lymph nodes. Follow-up examination every four weeks after the treatment for a total of six month period, physical checkup and CT of the patient showed no signs of tumor mass were found after treatment and the patient was in good health living a normal life for 2 years without any sign of metastasis.

Landscape of single cell transcriptome sequencing before and after lung cancer treatment

A total of 32918 cells were analyzed by scRNA-seq and we identified they belonged to 10 different cell types. Of which 8 cell types were found in tissue samples, namely B cells, basophils, Ecs, epithelial cells, fibroblasts, MPs, neutrophils, TandNK. There were 7 cell types in the blood samples, namely B cells, basophils, erythrocytes, MPs, neutrophils, platelets, TandNK. After treatment, the stromal cells in the tumor tissue decreased, and the TandNK cells increased. The neutrophils in the peripheral blood increased immediately after treatment and gradually decreased with the treatment time, and the TandNK cells, MPs, and B cells gradually increased. We also found that Chromosomes 6, 7, 17 all had obvious insertions, and Chromosomes 5, 7, 14, and 19 with obvious insertions and deletions (Figure 1 a, b, c).

Five neutrophil subpopulations were found in the blood samples, namely Neutrophils_1, Neutrophils_2, Neutrophils_3, Neutrophils_4 and Neutrophils_5. Among them, Neutrophils_2 increased significantly after treatment but gradually decreased with the time course of treatment; A subpopulation of Neutrophils_5 cells appeared from one week after treatment, and gradually increased. Neutrophils_1 cells had high expression of inflammation-related genes and chemokines CXCl8, PDE4B; Neutrophils_2 highly expressed arginase 1 (ARG1), and were significantly enriched for the signalling pathways related to the production of reactive oxygen species (glycolysis, oxidative phosphorylation), which will lead to the inhibition of T cell activation (Figure 2 a, d).

Immediately after treatment, a large number of neutrophils appeared in the body, producing an acute phase inflammatory response. After the treatment, neutrophils gradually returned to normal levels, neutrophils related to tumor development gradually decreased, and the proportion of neutrophils in the naïve state gradually increased (Figure 2 d).
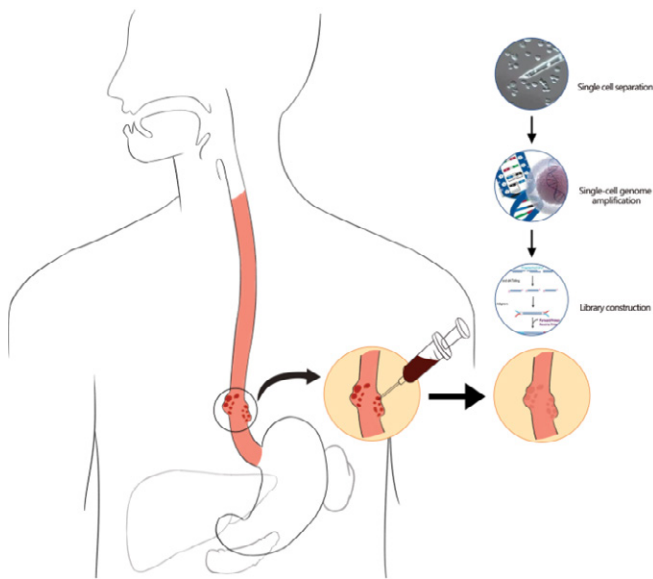
Figure 1: Graphic abstract of schematic diagram of single-cell sequencing process for esophageal cancer treatment during esophagectomy

a: Open the chest through the ribs, wash hands to explore the tumor, take a small piece of tumor as a untreated sample, then using syringe for injection of chemotherapy drug plus hapten into tumor area, in order to cause the tumor cell death, necrosis with inflammation, there is an haptenization with the tumor antigen released from death tumor cells be strong tumor antigens as neu tumor antigens (TAA) while DC cell capture the neu tumor antigens for antigen presentation process. After 1.5hour, cut off whole esophageal tumor and take another piece of tumor again for test as treated sample.

b: After DC cell capture the neu tumor antigens for antigen presentation process, the immune system of patient body produce the immunity reaction related whole body immunological response to tumor.
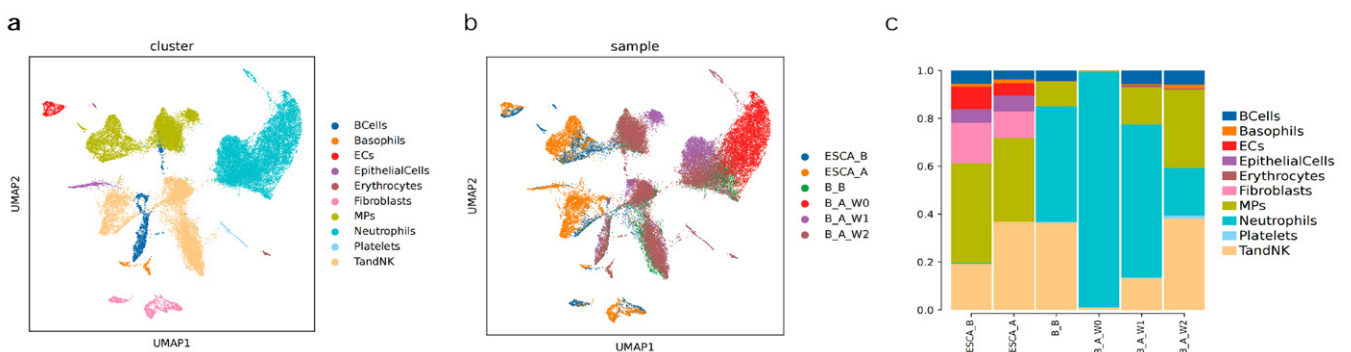
By scoring the HALLMARK_GLYCOLYSIS, Electron transport chain, and Oxidative phosphorylation pathways for each subset of neutrophils, we found that Neutrophils_2 and Neutrophils_5, which are at the front end of differentiation, had the highest scores. The expression in the 6 clusters of genes, Cluster_5 was significantly up-regulated after treatment, and gradually decreased over time. GO enrichment analysis showed that both the P38MAP signaling pathway and NADPH-related enzyme activities were significantly enriched. When inflammation occurs, these are the first sets of molecules that are recruited to the inflamed site (Figure2 c, e, f).

Changes of T and NK cells in blood before and after treatment during esophagectomy

T and NK cells have 8 subgroups: CD4NaiveT, CD8Tex, CD8NaiveT, GDT Cells, NK, Proliferating T, Teff, Treg. In peripheral blood samples, NK cells accounted for a large proportion (Figure 3 a,b). Through gene expression pattern clustering analysis, the gene set of expression pattern 6 was significantly up-regulated after treatment, and gradually decreased in the later stage of treatment (Figure 3 b). Through GO pathway enrichment analysis, it was enriched to NK cell-mediated cytotoxicity pathway; NK cells mediate immune response, activation of immune receptors, activation of neutrophils and other pathways. After one week of treatment, the proportion of GDT Cells increased. γδT cells are a group of special T cells. Although they account for a small proportion of T cells, they also play an important role in the immune system. One to two weeks after treatment, GDT cells in the peripheral blood showed up-regulated expression of Fc receptor-related signaling pathways and enhanced interaction with tumor cells through IFNG_Type II IFNR compared with before treatment (Figure 3 c,d,e).

Figure 2: Global transcriptome landscape of esophageal cancer before and after treated during of esophagectomy with hapten hanced intratumoral injection with cyctooxic drug plus hapten in total 32918 cell

a: Formation through dimensionality reduction clustering: formation of UMAPUMAPUMAPUMAP cell cluster through dimensionality reduction clustering, and a total of 10 cell types were obtained, including; Different colors represent cell types

b: Distribution of various cell types in tissues and blood before and after treatment, with different colors representing samples: Distribution of various cell types in tissues and blood before and after treatment, with different colors representing samples: The distribution of various cell types in tissue and blood before and after treatment, with different colors representing samples

c: Histogram of proportion of various cell types in tissue and blood samples before and after treatment: Histogram of proportion of various cell types in tissue and blood samples before and after treatment

Citation: Baofa, Yu, Jian Zhang, Hongzhu, Gao, Han Yan, Feng Gao, Peng Jing, Peicheng Zhang, Guoqin Zheng, Xiaomin Zhang. Immune Reaction Induced with Hapten Enhanced Intratumoral Chemotherapy during Esophagectomy:Explore Possible Immunosurgery. Journal of Cancer Science and Clinical Therapeutics. 8 (2024): 10-21.

Changes of MPs cells in blood before and after treatment during esophagectomy:

MPs are divided into 4 subgroups: cDC2, ClassicaMono, Macrophages, NonClassicaMono. Classical monocytes are divided into 5 subpopulations: ClassicaMono_1, ClassicaMono_2, ClassicaMono_3, ClassicaMono_4, ClassicaMono_5 (Figure 4 a, b, c, e). ClassicaMono_3 was mainly detected in tissue samples. KEGG enrichment results show that the cells of this subgroup are mainly enriched for inflammation-related signaling pathways (TNF signaling pathway, NFkB signaling pathway, etc.) and for HIF that is related to the microenvironment of tumor hypoxia -1 signaling pathway.

Expression pattern cluster analysis results showed that Cluster2 in blood was significantly up-regulated after treatment and gradually down-regulated over time. The enrichment analysis of this geneset showed that it was associated with neutrophil activation and related immunity. The proportion of cDC2 cells in tumor tissue samples increased slightly after treatment. Compared with before treatment, after treatment, antigen presentation and Toll-like receptor-related genes in cDC2 cells were all up-regulated (Figure 4 d, f, g, h).
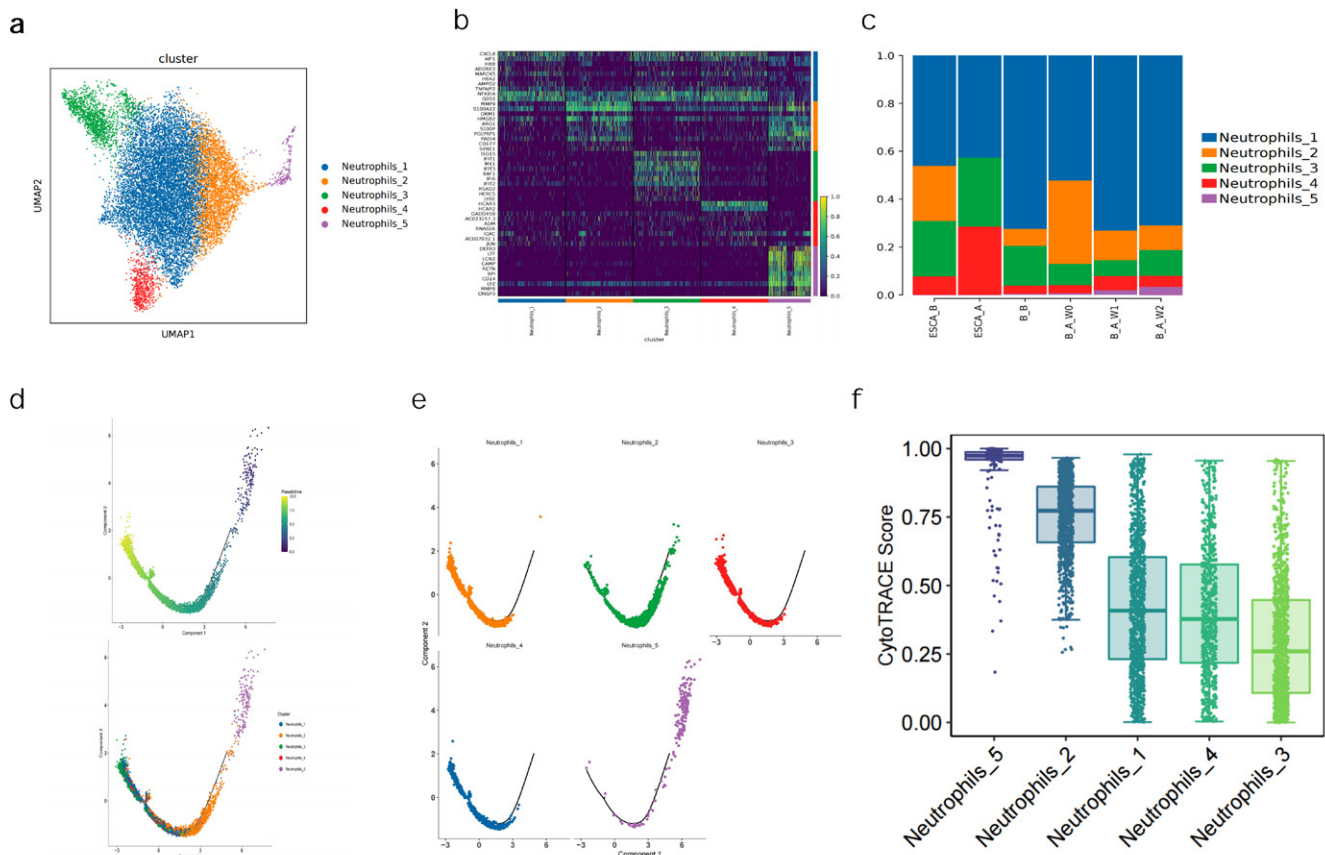

Figure 3: Changes of neutrophils cell composition in blood of patient's esophageal cancer before and after treatment during esophagectomy

a: Subgroup of neutrophils by dimensionality reduction clustering: Subgroup of neutrophils by dimensionality reduction clustering: Subgroup of neutrophils by dimensionality reduction clustering: Subgroups of neutrophils were performed, and UMAPUMAPUMAPUMAP cell cluster was formed through dimensionality reduction clustering. Cell cluster map was obtained, and 5 neutrophils subgroups, 1 neutrophils subgroup, and 1 neutrophils subgroup were obtained. There are subgroups of neutrophils, and there are subgroups of neutrophils in different colors

b: Heat maps showing the differential genes of different neutrophil subsets

c: Histogram of the proportion of each neutrophil subgroup in mass tissue and peripheral blood before and after treatment: Histogram of the proportion of each neutrophil subgroup in mass tissue and peripheral blood before and after treatment

d: Pseudo-time locus analysis of 5 subgroups of neutrophils. In the figure above, the dark starting point is the pseudo-time locus analysis of each subgroup gradually along the pseudointerval axis. In the figure above, the dark starting point is the pseudo-time locus analysis of each subgroup gradually along the pseudointerval axis. In the figure above, the dark color is the starting point of the transformation along the pseudoaxis to the light color direction, which corresponds to the overall presentation direction of the neutrophil subtype on the pseudotime axis in the figure below

e: Distribution of neutrophil subgroups on the pseudotimeline

F: Through CytotraceCytotraceCytotraceCytotraceCytotraceCytotrace Cytotrace potential analysis of neutrophils
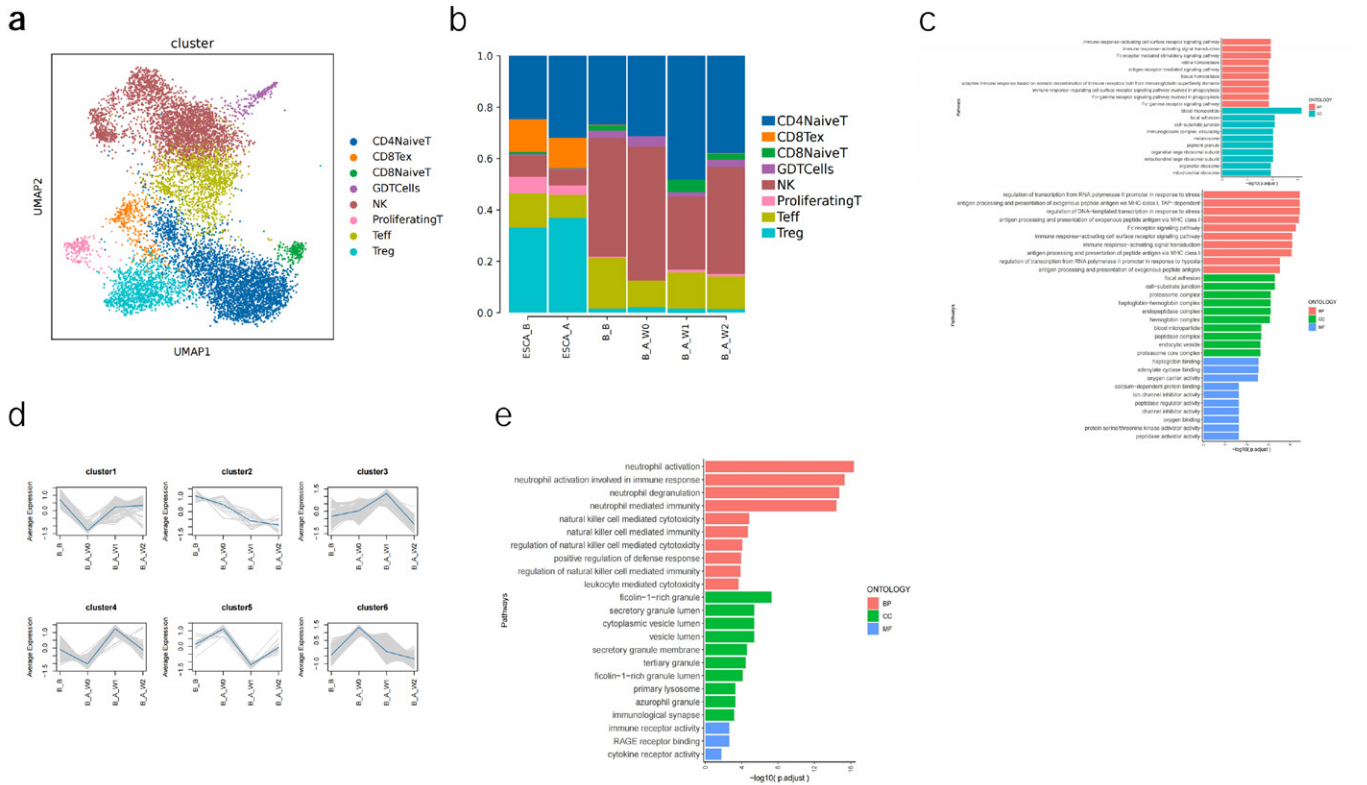

Figure 4: Changes of TandNK groups in patients with lung cancer before and after treatment during esophagectomy

a: Subgroup subdivision of TandNK cells was conducted, and UMAP cell cluster map was formed by dimensionality reduction clustering. A total of 8 TandNK cell subgroups were obtained, with different colors representing different subgroups

b: Histogram of proportion of each TandNK subgroup in mass tissue and peripheral blood before and after treatment

c: GO pathway enrichment analysis of GDTCells one week after treatment vs before treatment and two weeks after treatment vs before treatment

d: Genes with the same pattern expression (such as up-regulated expression over time) in NK cells were gathered together to form 6 patterns. e: GO pathway enrichment analysis was conducted on genes of cluster6 formed by gene expression pattern clustering in NK cells

Changes of EC cells in tumor tissue sample before and after treatment during esophagectomy

Five EC cells subtypes including AECs (arterial endothelial cells), CapECs (capillary endothelial cells), VECs (venous endothelial cells), TipCells (tip endothelial cells) and ProliferatingECs (proliferating endothelial cells) were found in the tumor tissue sample (Figure 5 a, b, e). Signaling pathways related to neutrophil activation and signaling pathways representing normal Ecs biological functions, such as protein kinase B signaling, were up-regulated, while signaling pathways related to cell adhesion and EC differentiation and development related to tumor development were down-regulated (Figure 5 c).

A large number of genes related to stress response are up-regulated, including some immediate early response genes (Immediate-Early Response Genes, IEGs, such as Fos, Jun, Junb, EGR1, Atf3, etc.). The heat shock protein family has the characteristic of naturally binding to various antigens, and can present antigen information to the immune system,

making it easier to recognize tumor cells. TipCells and ProliferatingECs are at the early stages of differentiation and have high differentiation potential, while AECs, CapECs and VECs are at a relatively late stages of differentiation. After treatment, the proportion of AECs, CapECs and VECs all decreased (Figure 5 d, f, g).

Changes of Fibroblasts cells in tumor tissue sample before and after treatment during esophagectomy

Four fibroblast subpopulation (Fibroblasts_1, Fibroblasts_2, Fibroblasts_3, Fibroblasts_4) and two parietal cell subpopulations (MuralCells_1 and MuralCells_2) were identified in tumor tissue sample respectively (Figure 6 a,b,d). The Fibroblasts_1 subpopulation also expressed high level of the chemokine CXCL14. Fibroblasts_2 is biased towards inflammatory fibroblasts, highly expresses the inflammation-related chemokines CXCL5, CXCL8, CXCL1, etc. After treatment, Fibroblasts_1 decreased significantly, and Fibroblasts_2/3/4 increased in varying degrees, with Fibroblasts_2 increasing most obviously (Figure 6 c, e).
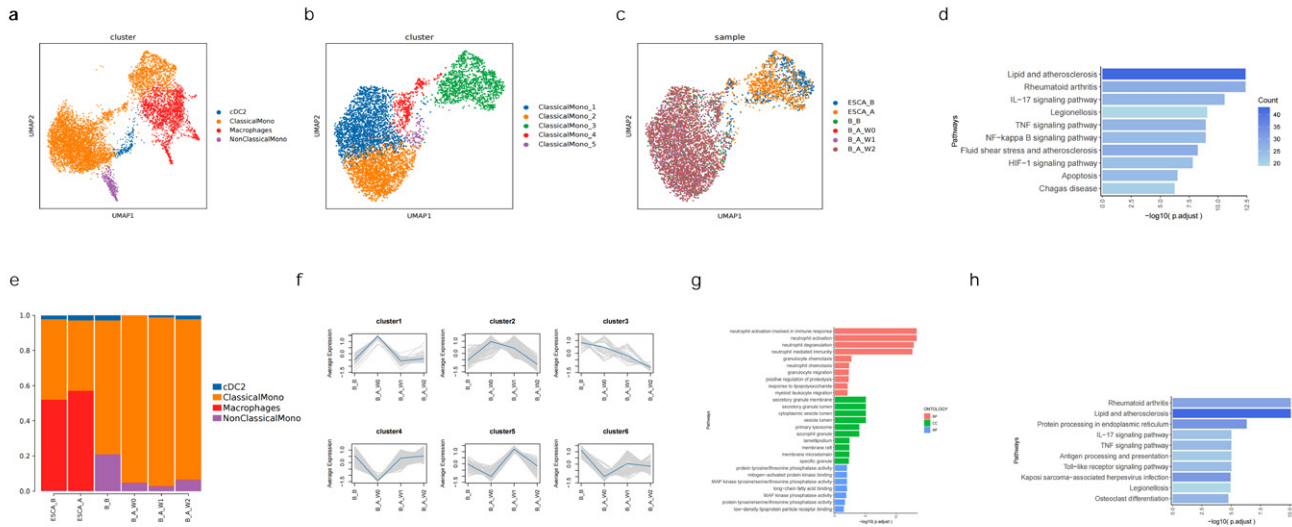
Figure 5: Changes of MPs groups in patients with lung cancer before and after treatment

a: Subgroup subdivision of MPs was conducted, and UMAP cell cluster map was formed by dimensionality reduction clustering. A total of 4 subgroups were obtained, with different colors representing different subgroups

b: Subgroup subdivision was carried out for ClassicaMono, and UMAP cell cluster map was formed by dimensionality reduction clustering. A total of 5 subgroups were obtained, with different colors representing different subgroups

c: Distribution of ClassicaMono subgroups in different samples. Different colors represent different samples

d: KEGG enrichment analysis was conducted for differential genes of ClassicaMono_3

e: Histogram of proportion of each MPs subgroup in mass tissue and peripheral blood before and after treatment

f: Genes with the same MPs pattern expression (such as up-regulated expression over time) were grouped together to form 6 patterns g: GO pathway enrichment analysis was conducted on cluster_2 obtained after clustering gene expression patterns

h: KEGG enrichment analysis was performed for up-regulated genes in cDC2 cells after treatment

Changes in the communication relationship between cells and significant changes in cytokine interaction

In tumor tissue samples, after treatment, the interaction between Fibroblasts and MPs and Neutrophils was strengthened, and MPs recruited a large number of neutrophils through CCL3-CCR3, CXCL1-CXCR2, CCL3-CXCR2 and CXCL8-CXCR2 (Figure 8 a). In the blood samples, immediately after treatment, the interaction between neutrophils and various immune cells became stronger. One week after treatment, the interaction between MPs and individual immune cells reached the strongest. After two weeks of treatment, TandNK, B cells play an interactive connection with each cell (Figure 7 b,c).

Discussion

The surgical treatment of esophageal cancer has been around for more than 100 years [1]. Although the treatment of early esophageal cancer is effective, for advanced esophageal cancer, the results of surgical treatment are no longer optimistic. Even if the tumor is removed at an advanced stage, the patient's survival time may not be extended, possibly due to cancer cell metastasis after surgery, but surgery can rapidly shrink tumor boundaries in favor of immunotherapies such as PD-1 or PD-l1 [6]. Our current study has demonstrated

that HEIC fusion in esophagectomy is a promising strategy in awake immune cells for preventing cancer metastasis and improving the treatment outcome. We used scRNA-Seq and demonstrated that HEIC fusion in esophagectomy induced acutely the appearance of 8 different cell types (Bcells, Basophils, Ecs, EpithelialCells, Fibroblasts, MPs, Neutrophils, TandNK) in the cancer tissues and 7 cell types in blood samples(Bcells, Basophils, Erythrocytes, MPs, Neutrophils, Platelets, TandNK). The TandNK cells increased; the neutrophils in the peripheral blood increased after treatment, and gradually decreased with the treatment time, and the TandNK cells, MPs, and BCells gradually increased. Our study also has also revealed insertions in Chromosomes 6, 7, 17, and both insertions and deletions in Chromosomes 5, 7, 14, and 19 (Figure 1). These findings are evidence for acute inflammation induced by surgery hapten-immunotherapy that likely contributes to suppression of tumor growth and metastasis [17, 18]. Among the neutrphils, Neutrophils_1 highly expressed inflammation-related genes and chemokines CXCl8, PDE4B; Neutrophils_2 highly expressed arginase 1 (ARG1), and significantly enriched for the signaling pathways related to the production of reactive oxygen species (glycolysis, oxidative phosphorylation), which will lead to the inhibition of T cell activation. In addition, the expression of S100 proteins S100A8, S100A9
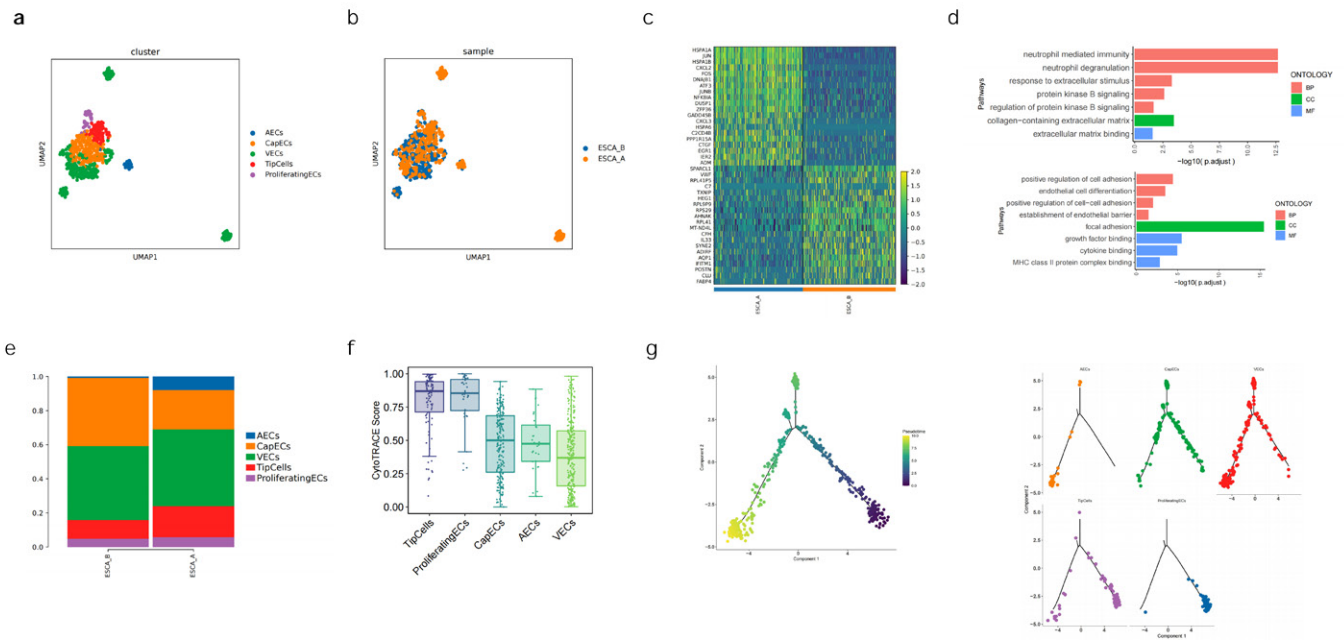
Figure 6: Changes of ECs cell of composition in patients with lung cancer before and after treatment

a: ECs are subdivided into subgroups, and UMAP cell grouping map is formed by dimensionality reduction clustering. A total of 5 subgroups are obtained, and different colors represent different subgroups.

b: Distribution of each subset of ECs in different samples, different colors represent different samples

c: heat map display of ECs differential genes before and after treatment

d: GO pathway enrichment analysis of up-regulated and down-regulated genes in ECs before and after treatment

e: Histogram of the proportion of each ECs subpopulation in tumor tissue before and after treatment

f: The differentiation potential of each ECs subset was analyzed by Cytotrace

g: Pseudo-time trajectory analysis of five subpopulations of ECs. The dark color is the starting point of differentiation, and gradually differentiates to the direction of light color along the false time axis, corresponding to the overall presentation of the ECs subtypes on the false time axis in the right picture

and MMP9 that activate vascular endothelial growth factor A (VEGFA) in the extracellular matrix in Neutrophils_2 is higher, which promotes and maintains tumor angiogenesis [31]; Neutrophils_3 highly expressed interferon (IFN)-stimulated genes, including ISG15, IFIT1/2/3 and RSAD2 [32]; Neutrophils_4 highly expressed niacin receptors HCR2 and HCR3, which is related to IFN-γ response [33]; Neutrophils_5 expressed DEFA3, DEFA4 and CD24, etc. It is a relatively immature neutrophil marker gene and has the highest differentiation potential [18, 34]. Previous studies have shown that neutrophils mainly obtain energy from glycolysis, and the expression of related metabolic gene sets is down-regulated after maturation [35]. When inflammation occurs, it is first recruited neutrophils to the inflamed site. However, due to the insufficient supply of glucose and oxygen at the inflammatory site, the neutrophils in the inflammatory site often need to use methods other than oxidative phosphorylation to generate energy, so as to meet the energy supply of neutrophils in the inflammatory state [36]. TandNK cells in the blood are very important for immune reaction, 8 subgroups(CD4NaiveT, CD8Tex, CD8NaiveT, GDTCells,

NK, ProliferatingT, Teff, Treg) are found in tumor tissue after treatment of HEIC immediately. In peripheral blood, NK cells accounted for a large proportion. GO pathway enrichment analysis showed that it was enriched for NK cell-mediated cytotoxicity pathway, NK cell-mediated Immune response, activation of immune receptors, activation of neutrophils and other pathways. In tumor immunity, γδT cells can migrate to the local tumor environment by recognizing NK cell receptors on the cell surface, and directly kill tumors by releasing cytotoxic substances such as perforin, granzymes, and cytokines (IFN-γ, TNF-α). These cells can also coordinate the activation of other cytotoxic T cells (NK cells, etc.) to achieve indirect killing of tumor cells [37]. In peripheral blood, GDTCells one week and two weeks after treatment showed up-regulated expression of Fc receptor-related signaling pathways and enhanced interaction with tumor cells through IFNG_Type II IFNR compared with before treatment.

MPs are divided into 4 subgroups: cDC2, ClassicaMono, Macrophages, NonClassicaMono. Classical monocytes usually infiltrate inflamed tissues, while atypical monocytes
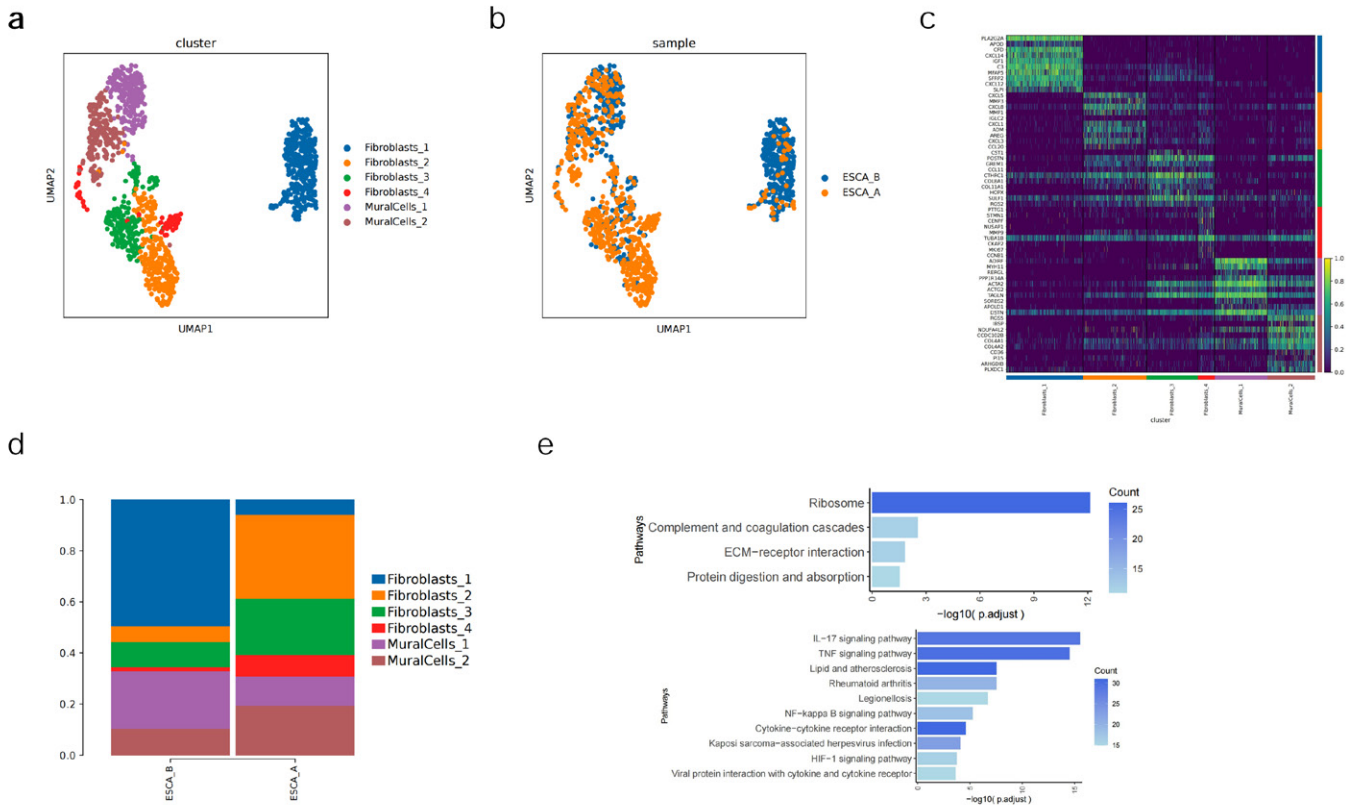
Figure 7: Changes of fibroblast composition in patients with lung cancer before and after treatment

a: Fibroblasts are subdivided into subpopulations, and the UMAP cell grouping map is formed by dimensionality reduction clustering. A total of 4 fibroblast subpopulations and 2 parietal cell subpopulations are obtained, and different colors represent different subpopulations

b: Distribution of each subpopulation of fibroblasts in different samples, different colors represent different samples

c: heat map display of differential genes in different fibroblast subpopulations

d: Histogram of the proportion of each fibroblast subset in tumor tissue before and after treatment

e: KEGG functional enrichment of two subpopulations, Fibroblasts_1 and Fibroblasts_2

usually play a role in immune surveillance in the blood [38]. Analysis of expression pattern clusters reveals that cluster2 in the blood sample was significantly up-regulated after treatment and gradually down-regulated over time. The enrichment analysis result of this gene set has showed that it was associated with neutrophil activation and related immunity. The proportion of cDC2 cells in tumor tissue samples increased slightly after treatment, antigen presentation and Toll-like receptor-related genes were all up-regulated. They may become memory T cells or B cells remain in the body forever. This is very important for initiate immunotherapy and makes it possible for immune surgery to be true. Fibroblasts also changed in tumor tissue sample before and after treatment during esophagectomy. We found four fibroblast subpopulations: Fibroblasts_1, Fibroblasts_2, Fibroblasts_3, Fibroblasts_4 and two parietal cell subpopulations are MuralCells_1 and MuralCells_2 in tumor tissue sample respectively. Fibroblasts_1 is enriched in ECM receptor-related signaling pathways and plays an

important role in promoting cancer cell motility and invasion [39]. A study on chemokines promoting breast cancer metastasis in the tumor microenvironment showed that the chemokine CXCL14 secreted by fibroblasts, as a marker of poor prognosis, plays a key regulatory role in the invasion and metastasis of breast cancer [40]. HEIC also induced five different endothelial cell subtypes: AECs (arterial endothelial cells), CapECs (capillary endothelial cells), VECs (venous endothelial cells), TipCells (tip endothelial cells) and ProliferatingECs (proliferating endothelial cells) in tumor tissue sample. A large number of genes related to immune stress response are up-regulated, including some immediate early response genes (Immediate-Early Response Genes, IEGs, such as Fos, Jun, Junb, EGR1, Atf3, etc.) and heat shock protein-related genes (HSPA1A, HSPA1B, HSP90, etc.) [41]. Deletion of Fos/Jun is the basis for the reduced immunostimulatory phenotype of TECs [42]. At present, heat shock protein therapy is also a hot development direction of tumor immunity [43]. A study on the heterogeneity of
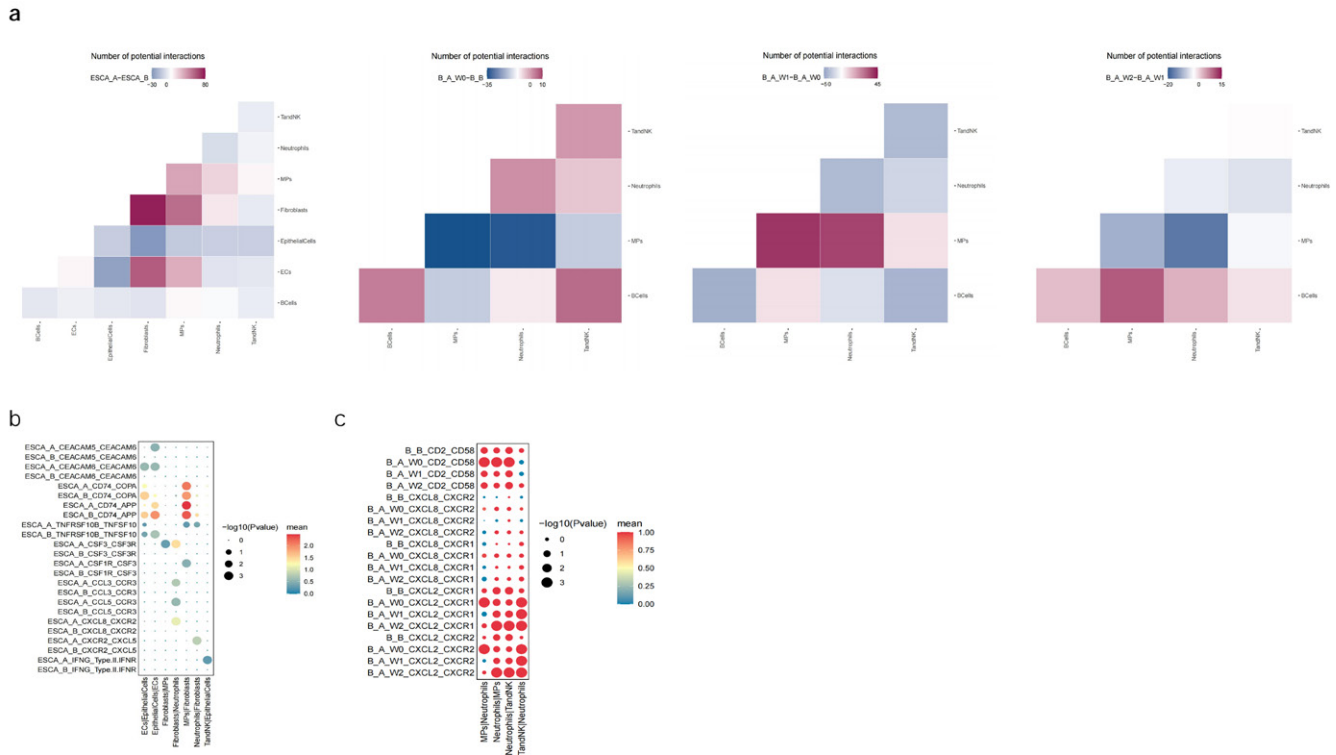
Figure 8: There is a strong link between cells in the communication relationship between cells and significant changes in cytokine interaction

a: ESCA_A vs ESCA_B, B_A_W0 vs B_B, B_A_W1 vs B_A_W0, B_A_W2 vs B_A_W1 cell communication difference map, red indicates that the former group interacts strongly, and blue indicates that the latter group interacts strongly

b: Significant differences between Fibroblasts, ECs, TandNK, Neutrophils, EpithelialCells (CancerCells) in the tissue mass before and after treatment

c: Significant differences between Neutrophils, MPs, and TandNK in blood samples before and after treatment

endothelial cells in cervical cancer showed that compared with normal samples, endothelial cells displayed more arterial, venous and capillary markers [42].

HEIC fusion in surgery also strengthened the interaction between fibroblasts and MPs and Neutrophils. MPs recruited a large number of neutrophils through CCL3-CCR3, CXCL1-CXCR2, CCL3-CXCR2 and CXCL8-CXCR2 [44]. Studies have shown that these genes have a negative impact on the prognosis of patients in the tumor microenvironment [45]. while CEACAM5 the interaction strength with CEACAM6 is up-regulated. According to reports, CEACM can transmit signals that produce multiple effects, including the activation of neutrophils and lymphocytes [18]. In summary, our current study shows that the interaction between TandNK cells, MPs cells, b cells, DC cells, AECs cells, CapECs cells and VECs cells is induced during HEIC fusion surgery, which promotes the expression of a large number of genes and leads to upregulation of immune response, while esophageal resection rapidly reduces the tumor load, it's effective for immunotherapy. Our study provides evidence that hapten + chemotherapy-mediated surgery can induce systemic immunity to cancer by initiating an initial immune response from the tumor site, thus achieving the desired clinical immunotherapy effect, and in fact, we move immunotherapy to the early frontier of any treatment, which may be called immunosurgery.

Conflict of Interest statement:

All of authors do not have any conflict interest for the study.

Translational relevance to the manuscript

This research is a useful practical and valuable for medical relevance. The study provides evidence to support possible precision immunesurgery during esophagectomy that can potentially be applied to all other solid tumors in order to prevention of cancer metastasis and recovery.

References

1. Wyld L, RA Audisio, and GJ Poston. The evolution of cancer surgery and future perspectives. Nature Reviews Clinical Oncology 12 (2015): 115-124.

2. Mo DC, Zi-Yu Liang, Long Chen, et al. Efficacy and safety of adjuvant therapy with PD-1/PD-L1 inhibitors in cancer. Exp Ther Med 24 (2022): 749.

3. Coccolini F, Matteo Nardi, Giulia Montori, et al. Neoadjuvant chemotherapy in advanced gastric and esophago-gastric cancer. Meta-analysis of randomized trials. Int J Surg 51 (2018): 120-127.

4. Gao P, Chengche Tsai, Yuchong Yang, et al. Intraoperative radiotherapy in gastric and esophageal cancer: meta-analysis of long-term outcomes and complications. Minerva Med 108 (2017): 74-83.

5. Wang Q, Jinyi L, Tao L, et al. Postoperative adjuvant chemotherapy versus chemoradiotherapy for node-positive esophageal squamous cell carcinoma: a propensity score-matched analysis. Radiat Oncol 15 (2020): 119.

6. Kim S I, Cassella C R, Byrne K T, et al. Tumor Burden and Immunotherapy: Impact on Immune Infiltration and Therapeutic Outcomes. Front Immunol 11 (2021): 629722.

7. Adair K, X Meng, and DJ Naisbitt. Drug hapten-specific T-cell activation: Current status and unanswered questions. PROTEOMICS 21 (2021): 2000267.

8. Al Qaraghuli MM, Soumya Palliyil, Gillian Broadbent, et al. defining the complementarities between antibodies and haptens to refine our understanding and aid the prediction of a successful binding interaction. BMC Biotechnology 15 (2015): 99.

9. Bandara NA, Cody D Bates, Yingjuan Lu, et al. Folate-Hapten–Mediated Immunotherapy Synergizes with Vascular Endothelial Growth Factor Receptor Inhibitors in Treating Murine Models of Cancer. Molecular Cancer Therapeutics 16 (2017): 461-468.

10. Berd D, Takami Sato, Henry C Maguire Jr, et al. Immunopharmacologic analysis of an autologous, hapten-modified human melanoma vaccine. J Clin Oncol 22 (2004): 403-415.

11. Yu B, Fu Q, Han Y. Awaken Immune Cells by Hapten Enhanced Intratumoral Chemotherapy with Penicillin Prolong Pancreatic Cancer Survival. J Cancer 14 (2023): 1282-1292.

12. Gao F, Peng J, Jian L, et al. Hapten-enhanced overall survival time in advanced hepatocellular carcinoma by ultro-minimum incision personalized intratumoral chemoimmunotherapy. J Hepatocell Carcinoma 2 (2015): 57-68.

13. Gefen T, Jacob V, Soliman K, et al. The effect of haptens on protein-carrier immunogenicity. Immunology 144 (2015): 116-126.

14. Jing P, Liu J, Li J, et al. Use of Hapten Combined Cytotoxic Drugs for Enhancing Therapeutic Effect in Advanced Stages of Pancreatic Cancer. Journal of Liver Research, Disorders & Therapy 1 (2015): 13-23.

15. Parker CW, J Shapiro, Milton K, et al. Hypersensitivity to penicillenic acid derivatives in human beings with penicillin allergy. J Exp Med 115 (1962): 821-838.

16. Schrand B, Emily Clark, Agata Levay, et al. Hapten-mediated recruitment of polyclonal antibodies to tumors engenders antitumor immunity. Nature Communications 9 (2018): 3348.

17. Yu B, Y Lu, Feng G, et al. Hapten-enhanced therapeutic effect in advanced stages of lung cancer by ultra-minimum incision personalized intratumoral chemoimmunotherapy therapy. Lung Cancer (Auckl) 6 (2015): 1-11.

18. Yu B, Fu Q, Han Y, et al. An Acute Inflammation with Special Expression of CD11 & CD4 Produces Abscopal Effect by Intratumoral Injection Chemotherapy Drug with Hapten in Animal Model. J Immunological Sci 6 (2022): 1-9.

19. Yu B, Fu Q. Drug Mixed by H2O2 Injection Intratumoral to turning an Extracellular Matrix into Autologous Coagulum as Drug Depot. Novel Research in Sciences 4 (2020).

20. Yang J, Xiguang Liu, Sai Cao, et al. Understanding Esophageal Cancer: The Challenges and Opportunities for the Next Decade. Frontiers in Oncology 10 (2020): 1727.

21. Napier KJ, M Scheerer and S Misra. Esophageal cancer: A Review of epidemiology, pathogenesis, staging workup and treatment modalities. World journal of gastrointestinal oncology 6 (2014): 112-120.

22. Herszényi L and Z Tulassay. Epidemiology of gastrointestinal and liver tumors. Eur Rev Med Pharmacol Sci 14 (2010): 249-258.

23. Huang FL and SJ Yu. Esophageal cancer: Risk factors, genetic association, and treatment. Asian J Surg 41 (2018): 210-215.

24. Betancourt-Cuellar SL, Marcelo F K Benveniste, Diana P Palacio, et al. Esophageal Cancer: Tumor-Node-Metastasis Staging. Radiol Clin North Am 59 (2021): 219-229.

25. Chen Z, Mengnan Z, Jiaqi L, et al. Dissecting the single-cell transcriptome network underlying esophagus non-malignant tissues and esophageal squamous cell carcinoma. EBioMedicine 69 (2021): 103459.

26. Kechin A, Uljana B, Alexander K, et al. cutPrimers: A New Tool for Accurate Cutting of Primers from Reads of

Targeted Next Generation Sequencing. J Comput Biol 24 (2017): 1138-1143.

27. Dobin A, Carrie A Davis, Felix S, et al. STAR: ultrafast universal RNA-seq aligner. Bioinformatics 29 (2013): 15-21.

28. Yu G, LG Wang, Y Han, et al. clusterProfiler: an R package for comparing biological themes among gene clusters. Omics 16 (2012): 284-287.

29. Efremova M, Miquel V-T, Sarah A T, et al. CellPhoneDB: inferring cell-cell communication from combined expression of multi-subunit ligand-receptor complexes. Nat Protoc 15 (2020): 1484-1506.

30. Qiu X, Andrew H, Jonathan P, et al. Single-cell mRNA quantification and differential analysis with Census. Nat Methods 14 (2017): 309-315.

31. Jaillon S, Andrea P, Diletta Di M, et al. Neutrophil diversity and plasticity in tumour progression and therapy. Nat Rev Cancer 20 (2020): 485-503.

32. Wang L, Yihao L, Yuting D, et al. Single-cell RNA-seq analysis reveals BHLHE40-driven pro-tumour neutrophils with hyperactivated glycolysis in pancreatic tumour microenvironment. Gut 72 (2023): 958-971.

33. Hughes TK, Tran D, Todd M G, et al. Second-Strand Synthesis-Based Massively Parallel scRNA-Seq Reveals Cellular States and Molecular Features of Human Inflammatory Skin Pathologies. Immunity 53 (2020): 878-894.

34. Schulte-Schrepping J, Nico R, Daniela P, et al. Severe COVID-19 Is Marked by a Dysregulated Myeloid Cell Compartment. Cell 182 (2020): 1419-1440.

35. Borregaard N and T Herlin. Energy metabolism of human neutrophils during phagocytosis. J Clin Invest 70 (1982): 550-557.

36. Sacks D, Blaise B, Bruce C V Campbell, et al. Multisociety Consensus Quality Improvement Revised Consensus Statement for Endovascular Therapy of Acute Ischemic Stroke. Int J Stroke 13 (2018): 612-632.

37. Silva-Santos B, S Mensurado and SB Coffelt. γδ T cells: pleiotropic immune effectors with therapeutic potential in cancer. Nat Rev Cancer 19 (2019): 392-404.

38. Amorim A, Donatella D F, Ekaterina F, et al. IFNγ and GM-CSF control complementary differentiation programs in the monocyte-to-phagocyte transition during neuroinflammation. Nat Immunol 23 (2022): 217-228.

39. Lochter A, S Galosy, J Muschler, et al. Matrix metalloproteinase stromelysin-1 triggers a cascade of molecular alterations that leads to stable epithelial-to-mesenchymal conversion and a premalignant phenotype in mammary epithelial cells. J Cell Biol 139 (1997): 1861-1872.

40. Sjöberg E, M Meyrath, Laura M, et al. A novel ackr2-dependent role of fibroblast-derived cxcl14 in epithelial-to-mesenchymal transition and metastasis of breast cancer. Clin Cancer Res 25 (2019): 3702-3717.

41. Denisenko E, Belinda B G, Matthew Jones, et al. Systematic assessment of tissue dissociation and storage biases in single-cell and single-nucleus RNA-seq workflows. Genome Biol 21 (2020): 130.

42. Li C, Luopei G, Shengli L, et al. Single-cell transcriptomics reveals the landscape of intra-tumoral heterogeneity and transcriptional activities of ECs in CC. Mol Ther Nucleic Acids 24 (2021): 682-694.

43. Yan X, Xiaojun Z, Yanzhong W, et al. Regulatory T-cell depletion synergizes with gp96-mediated cellular responses and antitumor activity. Cancer Immunol Immunother 60 (2011): 1763-1774.

44. Li E, Xiaobao Y, Yuzhang Du, et al. CXCL8 Associated Dendritic Cell Activation Marker Expression and Recruitment as Indicators of Favorable Outcomes in Colorectal Cancer. Front Immunol 12 (2021): 667177.

45. Wang X-d. The treatment of advanced stage primary liver carcinoma by local chemotherapy through hepatic artery and portal vein implantable drug delivery system combined with intratumor injection of ethanol. Journal of Clinical and Experimental Medicine (2006).